

## TABLE OF CONTENTS

<b>I Cases studied</b>	<b>2</b>
<b>1 DEM studies . . . . .</b>	<b>3</b>
1.1 DEM study: effective conductivity with disrupted packing . . . . .	3
1.1.1 Model Setup & Methodology . . . . .	3
1.1.2 Effective Thermal Conductivity from Analytic Analogy . . . . .	6
1.1.3 Results . . . . .	7
1.2 Conclusions . . . . .	15
<b>2 CFD-DEM studies . . . . .</b>	<b>17</b>
2.1 Pressure Drop . . . . .	17
2.2 Effective thermal conductivity from CFD-DEM . . . . .	17
2.2.1 Stagnant interstitial fluid . . . . .	17
2.2.2 Purge gas . . . . .	19
<b>References . . . . .</b>	<b>23</b>

**Part I**

# **Cases studied**

# CHAPTER 1

## DEM studies

The discrete element method (DEM) is used by many ceramic breeder researchers to model the interaction of individual pebbles in an ensemble in an effort to obtain a more detailed understanding of pebble beds than is possible with experimental measurements of effective properties. For example see Refs.<sup>1,2,5,7,11,12</sup>

### 1.1 DEM study: effective conductivity with disrupted packing

#### 1.1.1 Model Setup & Methodology

We analyze a three-dimensional pebble bed consisting of mono-dispersed particles of diameter  $d_p$ . The particles are constrained by rigid  $y - z$ -planes at locations of  $\frac{x}{d_p} = \pm 10$  (the walls of our container). There are periodic boundary conditions in the  $y$ -direction located at  $\frac{y}{d_p} = \pm 7.5$ . Gravity acts in the negative  $z$ -direction and the particles are resting on a rigid  $x - y$ -plane at  $z = 0$  (the floor of the container) and held from the top by an  $x - y$ -plane at  $\frac{z}{d_p} = 30$  (the roof of the container). We pack to  $\phi = 64\%$  and, given the volume, have 11000 particles. The volume was chosen to represent the long, tall, narrow channels seen in many solid breeder module designs.<sup>3,4,9</sup>

For this study, the material properties were chosen to represent lithium metatinatate pebbles. All the properties come from Ref.<sup>6</sup> They are summarized in Table 1.1

In the first attempt at packing pebbles into the system, we begin with a common starting point of a filled, lightly packed volume of 10 550 pebbles. We simulate pouring the pebbles

Table 1.1: Maximum load and nominal tension.

E (GPa)	$\nu$	k (W/m-K)	C (J/kg-K)	$\alpha$ (1/K)
126	0.24	2.5	1156	$15 \times 10^{-6}$

into the volume by initializing them into the system from a height of  $\frac{z}{d_p} \approx 50$  and allow them to fall under the influence of gravity (see Fig. 1.1). We pack the pebbles into a higher packing fraction by means of oscillating the walls as if the pebble bed were sitting on a vibrating plate. This was to imitate the vibration packing technique done in our experimental lab when testing pebble beds in the uniaxial compression test stand. The vibration scheme was able to slowly densify the packed bed but, owing to the very small timestep of the simulation, the simulation times were impractically large to approach a packing fraction greater than  $\phi = 60\%$ .

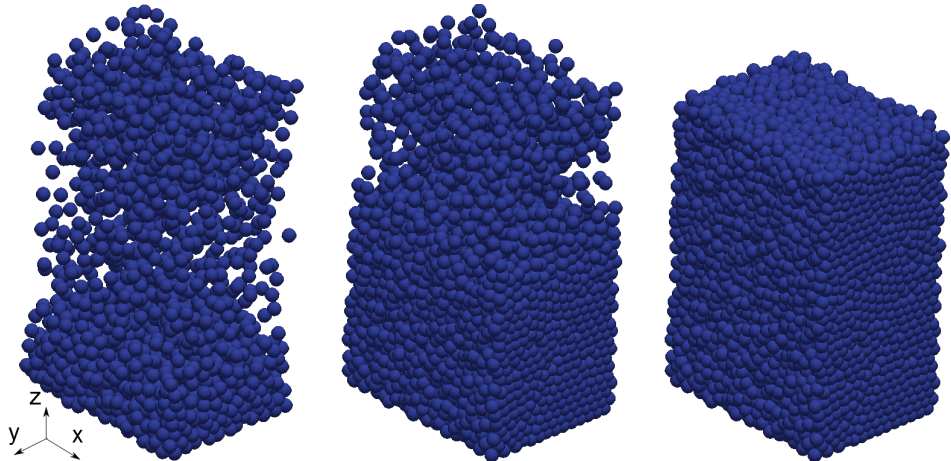


Figure 1.1: Demonstrating the pouring process of  $N = 10550$  pebbles into the control volume with at an early time (left), when it is nearly filled (middle) and after the pebbles have settled to negligible kinetic energy (right).

In the end, a simpler pack-relax method was used instead. In this method  $N$  particles are inserted into the volume such that we have precisely the packing fraction we desire (in this

case,  $\phi = 64\%$  so  $N = 11000$ ). The pebbles are placed at random into the volume and are allowed to artificially overlap – often by a great deal ( $\delta \sim R_p$ ). The overlap they experience would normally cause such an enormous force (integrating into an enormous velocity) that the pebbles would all explode out of the bed at the first step in time integration. We avoid such a catastrophic scenario with a relaxation scheme where we truncate the displacement of any pebble per timestep that is integrated from the force. The truncated displacement is very small and allows the pebbles to slowly move away from each other and into a static equilibrium as the artificial overlap is reduced. Once the pebble bed comes to rest, we remove the relaxation (limiting displacement command) and allow standard integration of contact forces with the velocity-Verlet algorithm (see ??). The pack-relax scheme allowed for obtaining desireable, highly repeatable packing fractions for all pebble beds. Once the pebble bed was packed into an initial condition, the simulation state was saved and used as a starting point for the numerous ‘crushed’ cases to be described later.

In this first study, we model pebble crushing without considering why the particular pebble should be cracking. In the model we randomly select pebbles from the ensemble, regardless of forces acting upon the pebble, and delete them entirely from the system. When a pebble is removed, the neighboring pebbles react due to the imbalance of forces, and the bed settles into a new configuration. We differentiated the failed beds by their percentage of failed pebbles:  $\eta = \text{number of failed pebbles per original ensemble size}$ . For the baseline case and for beds after failing, we apply the heating routine described next.

To simulate the conditions of a solid breeder in a fusion reactor, where the heat is removed from the pebble bed via contact to the containing structure, we assigned a constant temperature of  $T_c$  to the vertical walls. Nuclear heating of the pebbles is simulated through a constant source term on each pebble. A representative heating rate of  $Q_s = q''_p V_p$ , where  $q''_p = 8 \text{ MW/m}^3$ . The heating cycle runs until a thermal steady state is reached. Based on a measurement of the total thermal energy of the bed,  $E_T = \sum_i^N m_i C_i T_i$ , steady-state is determined as  $\frac{dE_T}{dt} = 0$  within a specified tolerance. Once at steady state, we analyzed thermal and mechanical characteristics of the pebble bed: effective thermal conductivity, average

coordination number, temperature profiles in the bed, and inter-particle contact forces.

Based on the boundary conditions to our system, we establish heat transfer that is symmetric and one-dimensional in the  $x$ -direction from  $x = 0$  to the walls at  $\frac{x}{d_p} = \pm 10$ . As we will show, the pebble bed has very little variation of forces and temperatures in the  $y$ -direction due to the periodic boundary condition at the edges of the domain. Gravity effects are minor in the overall heat transfer and induce only a slight  $z$ -dependency to the results. We take advantage of this nature of our pebble bed to find the effective conductivity from an analytic, one-dimensional test case.

### 1.1.2 Effective Thermal Conductivity from Analytic Analogy

Assuming a one-dimensional pebble bed, to find an effective conductivity, we step back into a continuum mechanics formulation where the pebble bed can be represented as a slab of solid material. We can analytically solve for the temperature equation in a slab with heat generation, symmetry about the centerline, and a constant boundary temperature condition.

At steady-state, the temperature of a material with constant temperature boundary conditions ( $T(L) = T_s$ ), constant thermal conductivity ( $k_{\text{eff}}$ ), and nuclear heating ( $q''$ ) obeys the following equation

$$0 = \frac{d^2T}{dx^2} + \frac{q''}{k_{\text{eff}}} \quad (1.1)$$

We introduce a non-dimensional temperature

$$\theta = \frac{T(x) - T_s}{T_0 - T_s} \quad (1.2)$$

where  $T_0$  is the temperature at the centerline of this slab (a value we will find momentarily).

The length is non-dimensionalized as

$$x^* = \frac{x}{L} \quad (1.3)$$

Thus we can re-write Eq. 1.1 as

$$0 = \frac{d^2\theta}{dx^{*2}} + G \quad (1.4)$$

where

$$G = \frac{q'''L^2}{k_{\text{eff}}(T_0 - T_s)} \quad (1.5)$$

In the non-dimensionalized form, the solution is revealed to be purely geometric,

$$\theta = 1 - x^{*2} \quad (1.6)$$

. as  $T_0 - T_s = \frac{q'''L^2}{2k_{\text{eff}}}$ . We will use the non-dimensional temperature solution of Eq. 1.6 to prove our one-dimensional assumption of heat transfer is justified for the pebble beds.

We note that in this continuum mechanics formulation, we are assuming that the nuclear source,  $q'''$  term is applied evenly over the entire volume. In our DEM formulation, our source term applies to a single pebble. To find the effective thermal conductivity of our ‘slab’ of pebble bed, we must reconcile this discrepancy. This is accomplished with the exchange of

$$q''' = \frac{Q_{\text{tot}}}{V_{\text{tot}}} = \frac{Q_s N}{H \cdot L \cdot W \cdot d_p^2} \quad (1.7)$$

where the pebble bed volume is given by the height,  $H$ , width,  $W$ , and length,  $L$ , and  $Q_s$  is the source term on each pebble in the DEM ensemble.

From the solution of Eq. 1.4, we find the effective conductivity to be

$$k_{\text{eff}} = \frac{q'''L^2}{2(T_0 - T_s)} \quad (1.8)$$

and when we replace the heat generation term with Eq. 1.7, and use the bed dimensions as given in § 1.1.1, this is written as

$$k_{\text{eff}} = \frac{Q_s N}{180(T_0 - T_s)d_p} \quad (1.9)$$

We will use this formulation of Eq. 1.9 to analyze and compare the pebble beds of this study.

### 1.1.3 Results

The aim of this study was both to discover the impact of pebble failure on thermomechanical properties as well as determine the impact as a function of the number of failed pebbles. To satisfy the latter, we created beds with  $\eta = 1\%, 3\%, 5\%, 10\%$ , and  $15\%$  of pebbles failed.

We plot Eq. 1.6 against the non-dimensionalized temperature profiles coming from the steady-state DEM simulation in Fig. 1.2. We find that all our models had a nearly perfect match to a one-dimensional prediction, validating the calculation of effective thermal conductivity in this study. Furthermore, the profiles adhering to the one-dimensional curve also allows us to find the effective conductivity of each bed from applying Eq. 1.9, which was derived from the one-dimensional assumption.

One concern we had for pebble crushing, was the phenomenon of ‘jamming’ during resettling that would possibly leave pebbles isolated from their neighbors (apart from those they are resting upon). Jamming can happen when a bridge of pebbles have a balance for forces without strong or any contact to a pebble below them. The pebble under the bridge then only has light contact with the pebbles upon which it is resting. Such an isolated pebble would have no strong pathway for heat transfer and heat up much higher than that of its neighbors. Evidence of pebble isolation is apparent in hot individual pebbles above the grouped curve in Fig. 1.2.

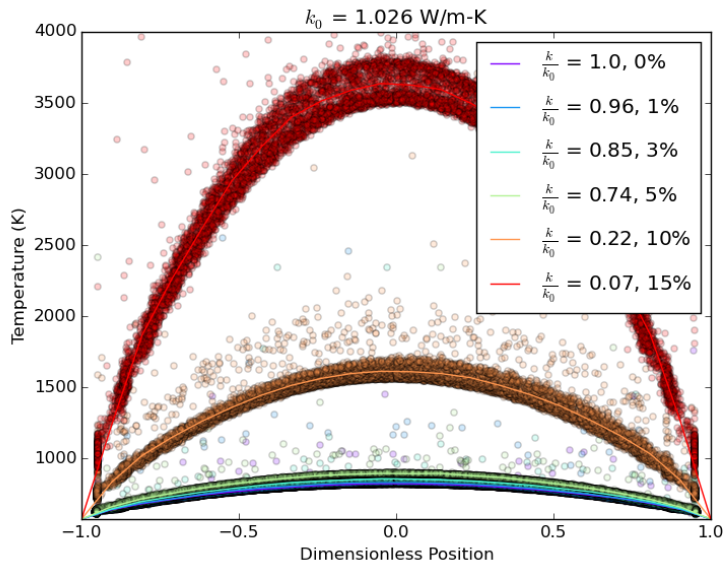


Figure 1.2: The nondimensional temperature profiles for each test case follow the theoretical shape of a one-dimensional, constant  $k$ , continuum solution.

The individual hot pebbles in Fig. 1.2 are also indicative of the shortcomings of the

discrete element method for modeling solid breeders in fusion reactors. The flowing purge gas in actual solid breeders would likely not permit such thermal isolation of pebbles. Even if a pebble had no physical contact with neighboring ones, it would still transport energy via conduction and advection of the helium gas. This will be addressed again and in more detail in § 2.2.

In order to calculate an effective conductivity of the pebble bed, we must find an average temperature profile through the bed to compare with Eq. 1.6 and thus employ Eq. 1.9. We compare steady-state temperature profiles in the test beds against the one-dimensional, non-dimensional temperature profile. Average values of the bed, along the  $x$  direction, are generated via averaging temperatures in bins. We create bins that are volumes slices of width  $\Delta x$  that extend through the limits of the  $y$ - and  $z$ -directions. We then find the  $n$  pebbles residing in the slices and take the mean value of their temperatures,

$$\langle T \rangle = \frac{1}{n} \sum_i^n T_i \quad (1.10)$$

Using the volume slices, we also find the average coordination number,

$$\langle Z \rangle = \frac{1}{n} \sum_i^n Z_i \quad (1.11)$$

and average contact force,

$$\langle F^{1/3} \rangle = \frac{1}{n} \sum_i^n F_{n,ij}^{1/3} \quad (1.12)$$

The effective thermal conductivity is found for all of our pebble beds, via Eq. 1.9, then normalized against the conductivity of the baseline ensemble ( $k^* = k/k_0$ ). Figure ?? shows the decreasing ETC with pebble failure. When 15% of the pebbles are crushed in a pebble bed, the ETC has fallen all the way to only  $k^* = 0.07$ . This large reduction is especially important in light of the already poor thermal management of virgin pebble beds that, even in helium environments, have been experimentally measured at only approximately 1 W/m-K (see, e.g., Refs.<sup>8,10</sup>). To find the cause of decrease in conductivity we make use of the inter-particle information provided by DEM tools instead of comparing macroscopic properties of packing fraction or external pressure.

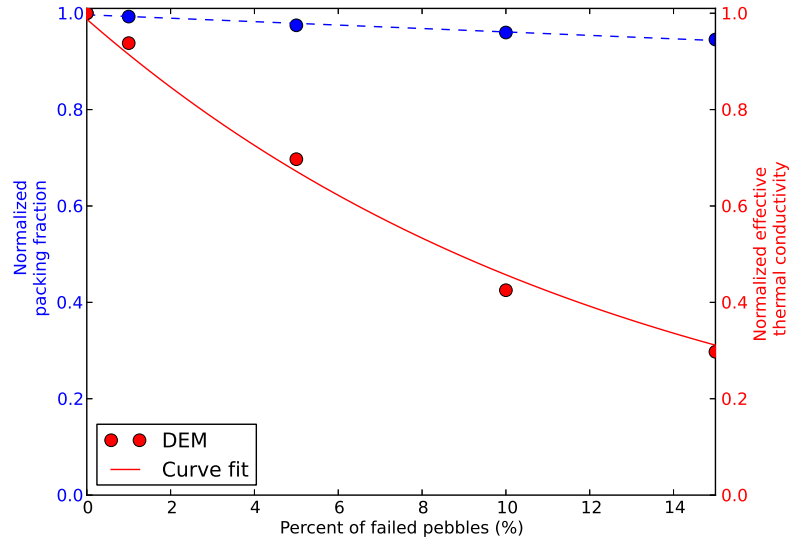


Figure 1.3: The normalized effective thermal conductivity (solid line) follows an exponential decay relationship with amount of failed pebbles. The normalized packing fraction (dashed line), compared to thermal conductivity, is relatively constant and is more closely fit to a linear reduction.

In Eq. ?? of ??, we see that at steady-state, the energy input by nuclear heating must be balanced by the transport of heat out of a pebble into its neighbors. Inter-particle heat transfer is dictated by the number of neighboring contacts, temperature difference between pebbles, and the thermal conductance,  $H_c$ , through the contact area. The thermal conductance (see Eq. ??) is itself a function purely of material properties (which are essentially constant here) and the force at the contact, going as  $H_c \propto F_{n,ij}^{1/3}$ . Thus, we write the net heat out of a pebble at steady state as a function of the three variables,

$$Q_{\text{net}} = f(Z, F_n^{1/3}, \Delta T) \quad (1.13)$$

The coordination number and contact forces are features of the packing structure in the packed bed that we can analyze to discover what happens to the heat flux between pebbles when the bed experiences crushed particles. Conversely, the  $\Delta T$  between two pebbles is the effect of the thermal transport (i.e. leading to higher bed temperatures such as those of Fig. 1.2). We will first analyze the changes to the coordination numbers of pebbles in the ensemble as pebbles crush.

- |                                      |                 |
|--------------------------------------|-----------------|
| (a) Baseline pebble bed (0% crushed) | (b) 1% crushed  |
| (c) 3% crushed                       | (d) 5% crushed  |
| (e) 10% crushed                      | (f) 15% crushed |

Figure 1.4: Caption

The average coordination number for the different pebble beds are shown in the plots of Fig. 1.4. Clearly, there are fewer contacts in the pebble bed after failure but this alone does not account for the reduction in  $k_{\text{eff}}$ . Next we look to the normal contact forces between pebbles in the bed.

The contact forces affecting  $Q_{\text{net}}$  for the different levels of crushed pebbles are plotted in Fig. 1.5. A dramatic reduction in the normal forces is seen after many of their neighbors are

crushed and are removed from the system. From the baseline down to the 15% failed case, the contact forces are reduced by about a factor of 10.

Another feature of Fig. 1.5 to point out is the change in distribution of average normal contact forces as the pebble beds experience crushed particles. For the well-packed beds of the baseline case up to the bed with 5% crushed pebbles, the contact forces are relatively evenly distributed through the bed (i.e. the binned average line is relatively flat). However as substantial numbers of pebbles are induced to be crushed for the 10% and 15% beds, we see more of a dependence on location for contact force. This is based on the massive re-arrangement that happens in these beds. To demonstrate, we view the pebble bed of the 15% crushed case in Fig. 1.6.

After 15% of the pebbles are removed from the system, a tremendous amount of resettling occurs and a large gap appears between the top wall and the top layer of pebbles. When heating is applied, the pebbles heat up very high until such time that they swell and press into each other with enough force to allow sufficient heat to conduct between them to balance the nuclear heating. Because of the resettling tending collapse toward the center, the residue of the resettling is apparent in the average normal contact forces of Fig. 1.5f.

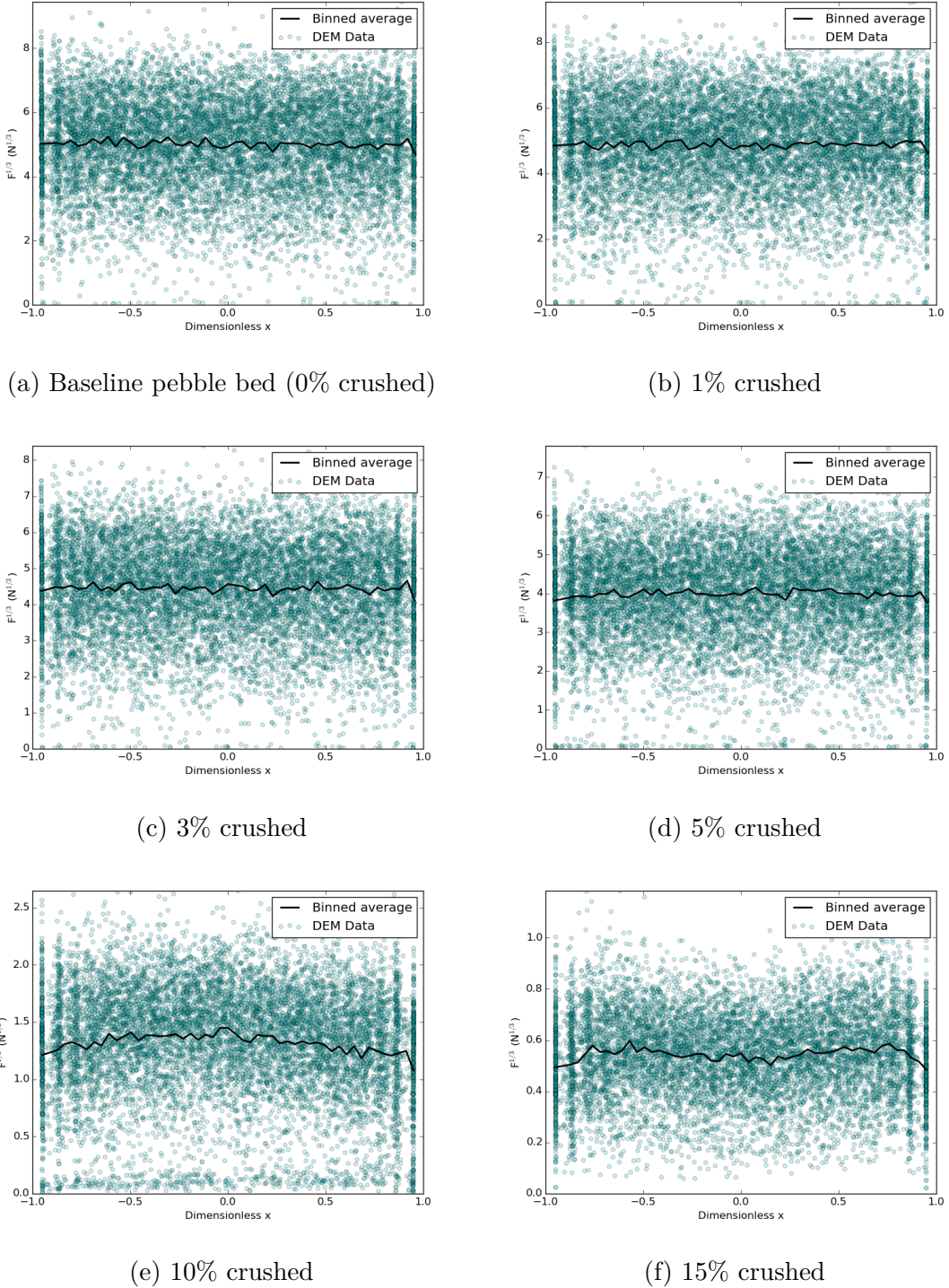
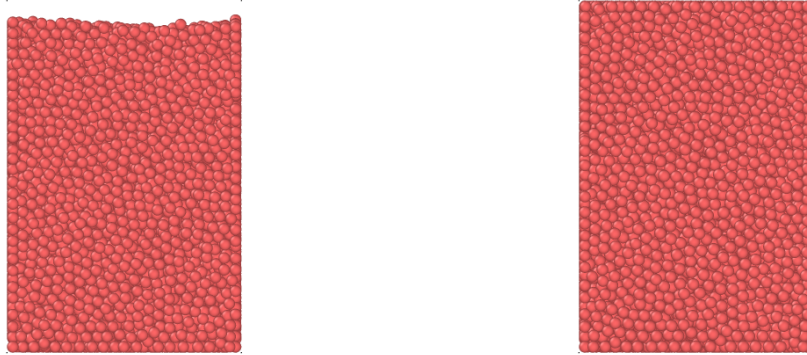


Figure 1.5: As pebble beds experience massive amounts of crushed pebbles ( $>5\%$ ), the contact forces in the ensemble (after heating to steady-state) show dramatic reductions in value. Note the change of scale on the figures from the baseline case to the 15% crushed case.



(a) Side-view of the pebble bed after reset- (b) Side-view of the pebble bed after heating  
tling from the crushing event, before heating.

Figure 1.6: In (a) we see the pebble bed after 15% of the pebbles have been crushed (removed) and then after the heating cycle in (b). The gap formed after crushing is completely filled by swelling pebbles.

## 1.2 Conclusions

The results shown in Figs. 1.5 and 1.4 demonstrate that the heat transfer through a pebble bed is simultaneously a function of both the coordination number and inter-particle contact forces. The average values of both of these parameters reduced as pebbles in the bed were crushed. Interestingly, when a pebble bed has lower overall inter-particle contact forces such as what we see when pebbles are crushed, we would predict fewer pebbles are likely to break. This result implies that pebble breakage is self-dampening; as pebbles begin to break the ensemble quickly relaxes and avoids future pebble failure. So while in this study we induced failure up to  $\eta = 15\%$  without a concern for predicting if such a large amount would break, such large values may not occur in real beds during operation of a fusion reactor.

The first study of this dissertation established the groundwork of the DEM modeling to be carried out in the other studies. We simulated a pebble bed with a specified fraction of the pebbles crushing during operation; then determining the repercussions of the missing pebbles as they affect the macroscopic property of effective thermal conductivity. We used the assumption of homogeneous, random locations of pebble failure to induce a failure routine without requiring external loads on the bed to actually induce the pebble crushing. After heating to a steady-state, an effective thermal conductivity was calculated for the pebble bed. The results show that large amounts of pebble failure correspond to large decreases in the conductive transport of energy through the pebble bed. The increase was due primarily to a drop in the inter-particle forces which lead to a large increase in temperature differences between neighboring pebbles.

As the first step in the modeling effort, there were many simplifications that had to be made in this study. We must note here the shortcomings of the assumptions and simplifications of this study before drawing any major conclusions from the results.

First, the ‘container walls’ surrounding the pebble bed in this model are completely rigid and do not react as the swelling pebble bed presses into them while heating. The confined thermal expansion leads to very high contact forces in the pebble bed that may not be

realistic. The abnormally high contact forces are most likely to be the source of the abnormally high baseline effective thermal conductivity,  $k_0 = 1.03 \text{ W/m-K}$ . In experiments on the effective thermal conductivity of lithium ceramics in vacuum, the beds are often allowed to expand freely while heating (in at least one direction) and in vacuum were measured to be closer to  $k_0 = 0.5 \text{ W/m-K}$  [FIND THE REAL VALUES TO PUT HERE!]. We note, however, that this value has been calculated in the absence of interstitial gas so the results apply only to the reduction in energy transferred via inter-particle conduction.

Second, we saw from Fig.1.2 that the majority of the pebbles in the ensemble have their temperatures close fitting to an average curve but a number of the pebbles had less thermal contact with neighboring particles and consequently had much larger temperatures. This was true even in the baseline case of a tightly packed ( $\phi = 64\%$ ) pebble bed. This phenomena is only possible because the contribution to heat transfer of the interstitial gas was not considered in this model. The flowing helium gas is expected to prevent any runaway temperatures of individual pebbles as it provides another route of energy transfer in the bed. This will be addressed in § 2.

# CHAPTER 2

## CFD-DEM studies

### 2.1 Pressure Drop

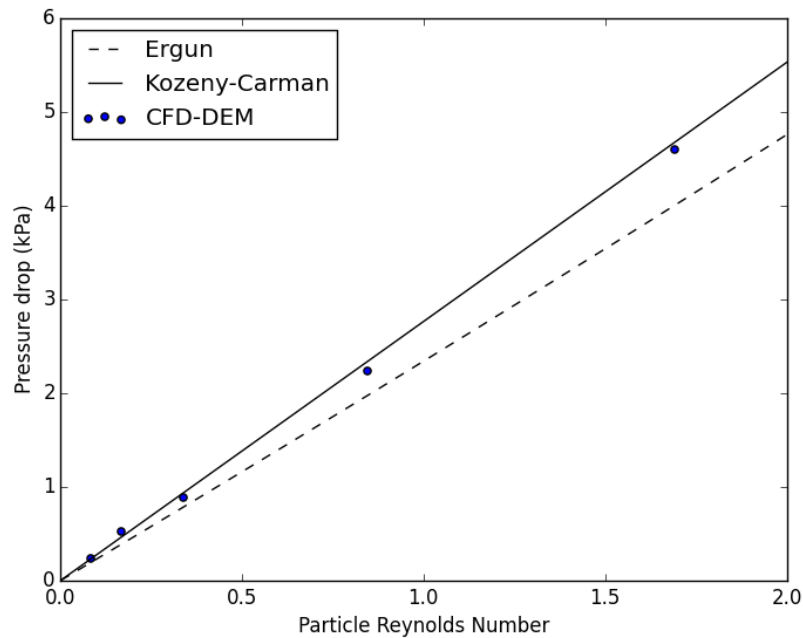
Before analyzing thermal results from the CFD-DEM coupling, the system was run at various particle Reynolds numbers and the overall pressure drop of the packed bed was measured. This value was compared against the well-known Kozeny-Carman and Ergun equations. The Kozeny-Carman is known to fit better with experimental data at very small Reynolds numbers. In Fig. 1 we see the CFD-DEM coupling model is providing bed-scale pressure drops that match very well with Kozeny-Carman over the Reynold's numbers applicable to helium purge flow in fusion reactors.

The flow is visualized in Fig. 2. The pebble bed is clipped at the centerline to allow viewing of the helium streamlines. Apparent in the figure is temperature profiles in the helium from centerline to wall that qualitatively mirror temperature profiles in the pebble bed.

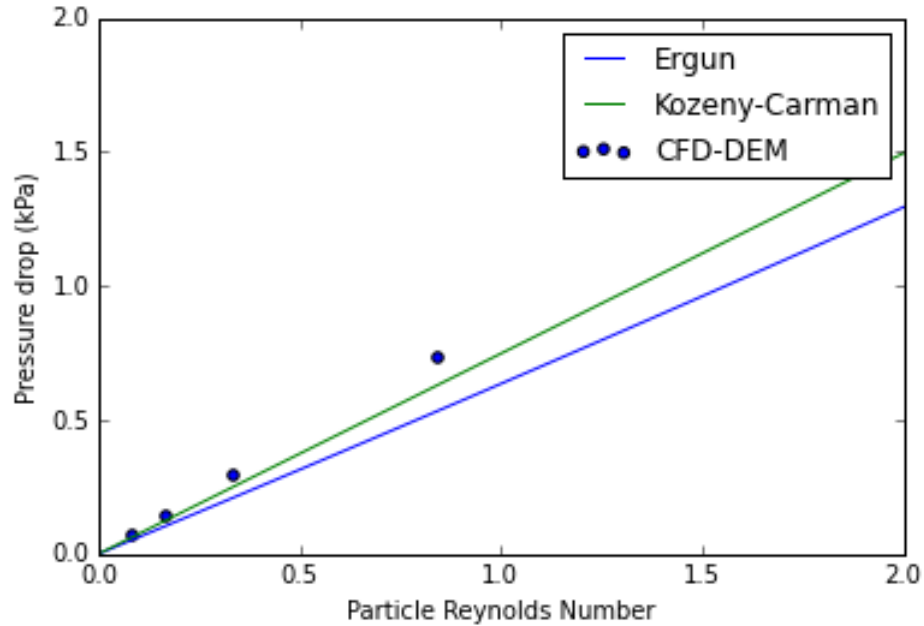
### 2.2 Effective thermal conductivity from CFD-DEM

#### 2.2.1 Stagnant interstitial fluid

can use correlations for stagnant gas in packed bed.



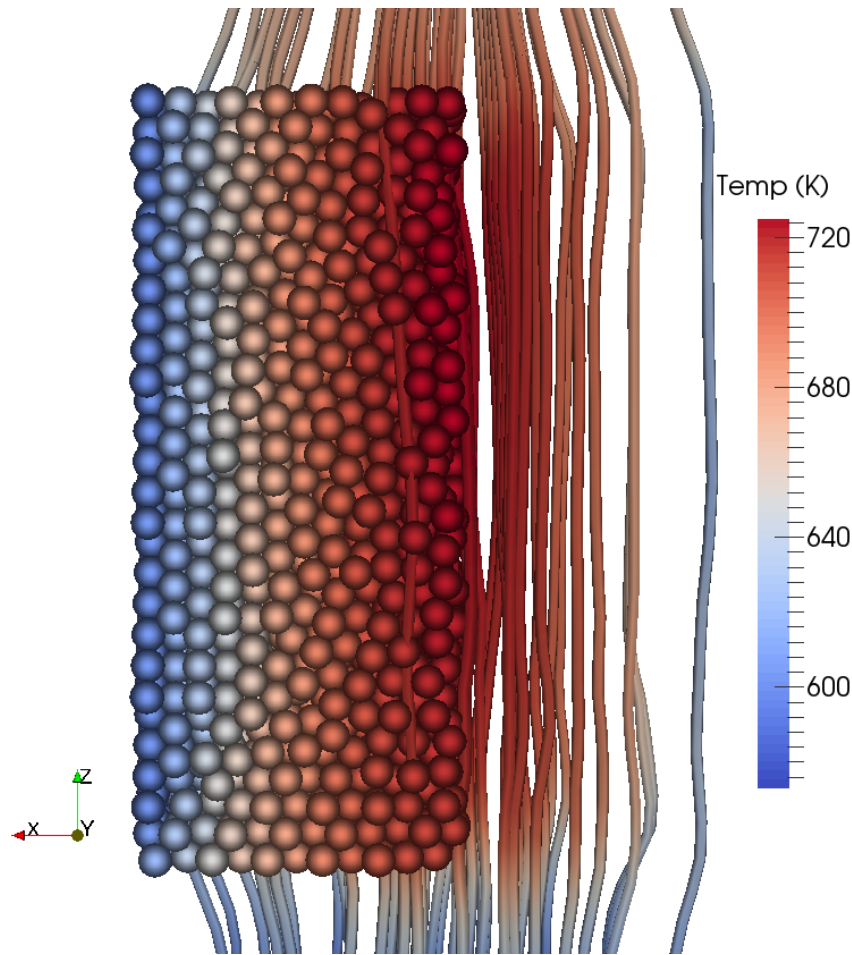
(a) Well-packed bed



(b) Re-settled bed

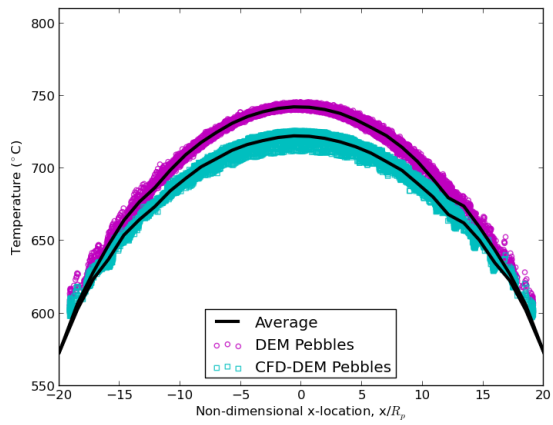
Figure 2.1: Pressure drop calculations across packed beds, solved by CFD-DEM, fit well to the Kozeny-Carman empirical relation.

Figure 2.2: Cut-away view of the pebble bed with streamlines of helium moving in generally straight paths from inlet to exit.

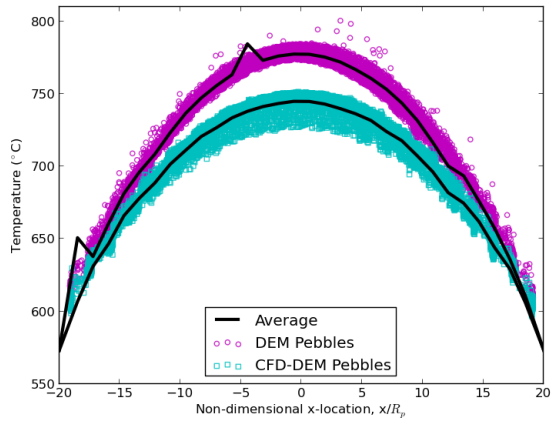


### 2.2.2 Purge gas

The well-packed and resettled pebble beds were run to thermal steady-state with nuclear heating and wall cooling in both pure DEM and coupled CFD-DEM simulations for comparison. From steady-state temperature distributions, seen in the pebble scatter plots in Fig. 3, an average profile is calculated and an effective thermal conductivity computed. The values are tabulated in Table I. In the case of pure DEM, energy is transported solely along conduction routes in the ensemble. When the packing of the bed is disturbed, this results in a substantial drop in effective conductivity (a drop of 31%). The details of the conductivity reduction were studied extensively in Ref. 23. Perhaps more important than the reduction



(a) Well-packed bed



(b) Re-settled bed

Figure 2.3: Scatter temperature profiles of pebbles in a bed that is: well-packed (left) and resettled after 10% of pebbles were removed from crushing (right). The introduction of helium into the simulation contributes to both lower overall temperatures (higher effective conductivity) and the smoothing out of high temperatures of isolated pebbles.

in effective conductivity, is the appearance of isolated pebbles. Because heat deposition is volumetrically applied, pebbles with poor conduction routes become much hotter than their neighbors. This is evident in the high temperatures seen in many of the pebbles in the right figure of Fig. 3. Over-heating of isolated pebbles could induce sintering and impact their tritium release even when the average temperatures measured in the bed are well below sintering values. When CFD-DEM beds are analyzed, there is still a large reduction in effective conductivity (22% drop), but interesting to note is the lack of isolated pebbles with high temperatures. In the CFD-DEM scatter plot of the right image in Fig. 3, there is evidence of the reduced heat transfer in the same region as the isolated pebbles from the DEM bed, but the temperatures are much closer to the average values of neighboring pebbles. The helium purge gas has effectively smoothed out the temperatures and provided heat transport paths for any pebbles that have loose physical contact with neighbors. In spite of the 22% decrease in effective conductivity, the maximum temperature of the pebble bed only increased 6.2% (from 725 to 751 K) when helium is included in the model. This result is significant for solid breeder designers. They may choose a solid breeder volume such that in the event of extensive pebble cracking, the maximum temperature of the bed would remain within the ideal windows dictate for the lithium ceramics.

Table 2.1: Pebble bed values from the test matrix of the beds analyzed in this study.

	$k_{\text{eff}}$ (W/mK)		$T_{\max}$ (K)		$\frac{Q_h}{Q_{\text{nuc}}}$
	DEM	CFD-DEM	DEM	CFD-DEM	CFD-DEM
Well-packed	0.96	1.09	745	725	1.15
Resettled	0.66	0.85	800	751	1.52

An accompanying result is the increased amount of energy carried out of the system by the helium purge gas. In Table I, the last column provides the ratio of energy carried out of the system to the nuclear energy deposited into the bed. The amount of energy carried out by the helium increased from 1.15% to 1.52% from ‘well-packed’ to ‘resettled’. evap-x-T-

color. The CFD-DEM formulation maintains calculations of pebble-pebble interactions while dynamically coupling to the helium flow. The model demonstrates the ability of helium gas to smooth out any hot spots predicted by pure-conduction DEM formulations. Further, the lattice-Boltzmann simulation, while not fully coupled to DEM, revealed important features of helium flow in volumetrically heated pebble beds – mainly the smearing of temperature profiles along the paths of cooling.

## REFERENCES

- [1] Zhiyong An, Alice Ying, and Mohamed A Abdou. Numerical characterization of thermo-mechanical performance of breeder pebble beds. *Journal of Nuclear Materials*, 367-370:1393–1397, 2007.
- [2] Ratna Kumar Annabattula, Yixiang Gan, Shuo Zhao, and Marc Kamlah. Mechanics of a crushable pebble assembly using discrete element method. *Journal of Nuclear Materials*, 430(1-3):90–95, November 2012.
- [3] Seungyon Cho, Mu-Young Ahn, Duck Hoi Kim, Eun-Seok Lee, Sunghwan Yun, Nam Zin Cho, and Ki Jung Jung. Current status of design and analysis of Korean Helium-Cooled Solid Breeder Test Blanket Module. *Fusion Engineering and Design*, 83(7-9):1163–1168, December 2008.
- [4] Mikio Enoeda, Y. Kosaku, Toshihisa Hatano, T. Kuroda, N. Miki, T. Honma, Masato Akiba, S. Konishi, H. Nakamura, Y. Kawamura, S. Sato, K. Furuya, Y. Asaoka, and Kunihiko Okano. Design and technology development of solid breeder blanket cooled by supercritical water in Japan. *Nuclear Fusion*, 43:1837–1844, 2003.
- [5] Yixiang Gan and Marc Kamlah. Discrete element modelling of pebble beds: With application to uniaxial compression tests of ceramic breeder pebble beds. *Journal of the Mechanics and Physics of Solids*, 58(2):129–144, February 2010.
- [6] Paul J Gierszewski. Review of properties of lithium metatitanate. *Fusion Engineering and Design*, 39-40:739–743, September 1998.
- [7] Zi Lu. *Numerical Modeling and Experimental Measurement of the Thermal and Mechanical Properties of Packed Beds*. PhD thesis, University of California Los Angeles, 2000.
- [8] G Piazza, Jörg Reimann, E Günther, Regina Knitter, N. Roux, and J D Lulewicz. Characterisation of ceramic breeder materials for the helium cooled pebble bed blanket. *Journal of Nuclear Materials*, 307-311(0):811–816, December 2002.
- [9] Y Poitevin, Lorenzo Boccaccini, M Zmitko, I Ricapito, J.F. Salavy, E. Diegele, F. Gabriel, E. Magnani, H. Neuberger, R. Lässer, and L. Guerrini. Tritium breeder blankets design and technologies in Europe: Development status of ITER Test Blanket Modules, test & qualification strategy and roadmap towards DEMO. *Fusion Engineering and Design*, 85(10-12):2340–2347, December 2010.
- [10] Jörg Reimann and S Hermsmeyer. Thermal conductivity of compressed ceramic breeder pebble beds. *Fusion Engineering and Design*, 61-62:345–351, November 2002.
- [11] Jon T. Van Lew, Alice Ying, and Mohamed Abdou. A discrete element method study on the evolution of thermomechanics of a pebble bed experiencing pebble failure. *Fusion Engineering and Design*, 89(7-8):1151–1157, October 2014.

- [12] Shuo Zhao. *Multiscale Modeling of Thermomechanical Properties of Ceramic Pebbles*. PhD thesis, Karlsruhe Institute of Technology, 2010.